Nat. Hazards Earth Syst. Sci. Discuss., 2, 1671–1692, 2014
www.nat-hazards-earth-syst-sci-discuss.net/2/1671/2014/
doi:10.5194/nhessd-2-1671-2014
© Author(s) 2014. CC Attribution 3.0 License.

Natural Hazards and Earth System Sciences
Open Access
Discussions

This discussion paper is/has been under review for the journal Natural Hazards and Earth System Sciences (NHESS). Please refer to the corresponding final paper in NHESS if available.

Spatial and seasonal responses of precipitation in the Ganges and Brahmaputra river basins to ENSO and Indian Ocean dipole modes: implications for flooding and drought

M. S. Pervez[1,2] and G. M. Henebry[2]

[1]ASRC Federal InuTeq, contractor to U.S. Geological Survey, Earth Resources Observation and Science (EROS) Center (Work performed under USGS contract G13PC00028), 47914 252nd Street, Sioux Falls, South Dakota 57198, USA
[2]Geographic Information Science Center of Excellence (GIScCE) South Dakota State University, 1021 Medary Ave., Wecota Hall 506B, Brookings, SD 57007-3510, USA

Received: 25 November 2013 – Accepted: 22 January 2014 – Published: 20 February 2014

Correspondence to: M. S. Pervez (spervez@usgs.gov)

Published by Copernicus Publications on behalf of the European Geosciences Union.

Abstract

We evaluated the spatial and temporal responses of precipitation in the basins as modulated by the El Niño Southern Oscillation (ENSO) and Indian Ocean (IO) dipole modes using observed precipitation records at 43 stations across the Ganges and Brahmaputra basins from 1982 to 2010. Daily observed precipitation records were extracted from Global Surface Summary of the Day dataset and spatial and monthly anomalies were computed. The anomalies were averaged for the years influenced by climate modes combinations. Occurrences of El Niño alone significantly reduced (60 % and 88 % of baseline in the Ganges and Brahmaputra basins respectively) precipitation during the monsoon months in the northwestern and central Ganges basin and across the Brahmaputra basin. In contrast, co-occurrence of La Niña and a positive IO dipole mode significantly enhanced (135 % and 160 % of baseline respectively) precipitation across both basins. During the co-occurrence of neutral phases in both climate modes (occurring 13 out of 28 yr), precipitation remained below average to average in the agriculturally extensive areas of Haryana, Uttar Pradesh, Bihar, eastern Nepal, and the Rajshahi district in Bangladesh in the Ganges basin and northern Bangladesh, Meghalaya, Assam, and Arunachal Pradesh in the Brahmaputra basin. This pattern implies that a regular water deficit is likely in these areas with implications for the agriculture sector due to its reliance on consistent rainfall for successful production. Major flooding and drought occurred as a consequence of the interactive effects of the ENSO and IO dipole modes, with the sole exception of extreme precipitation and flooding during El Niño events. This observational analysis will facilitate well informed decision making in minimizing natural hazard risks and climate impacts on agriculture, and supports development of strategies ensuring optimized use of water resources in best management practice under changing climate.

CC BY

1 Introduction

The phenomenon of the El Niño Southern Oscillation (ENSO) and its corresponding influences on regional precipitation are well studied and well documented even at a global scale (Ropelewski and Halpert, 1996). In the Asia-Pacific region, the ENSO signals are well linked with precipitation over Southern and Eastern Asia (Kumar et al., 1999; Wu and Wang, 2002) by modulating the Walker circulation (Kumar et al., 1999; Chowdhury and Ward, 2004). More specifically, the NIÑO3 Surface Temperature (SST) anomalies inversely correlate with precipitation in the Ganges and Brahmaputra basins and can explain 40 % ($p < 0.0001$) and 20 % (p=0.009) of the variation observed in the precipitation of the Ganges and Brahmaputra basins, respectively (Pervez and Henebry, 2013). The Indian Ocean (IO) dipole mode (Saji et al., 1999; Webster et al., 1999), accounting for 12 % of the SST variation in the IO, also influences precipitation over India (Ashok and Saji, 2007). However, the influence of these climate modes is not spatially uniform. Using two new IO dipole mode indices tuned for the Ganges and Brahmaputra basins, we have demonstrated that (i) the tropical west–east differential heating summarized in the Dipole Mode Index ($DMI_{west–east}$) in the Indian Ocean influences Ganges precipitation and (ii) the north–south differential heating summarized in $DMI_{north–south}$ in the Indian Ocean influences Brahmaputra precipitation (Pervez and Henebry, 2013). According to the Intergovernmental Panel on Climate Change's Fifth Assessment Report on the physical basis of climate change, the DMI will likely remain active and El Niño events may likely intensify because of a warming climate (Stocker et al., 2013); therefore, the influence of these climate modes on precipitation in South Asia is likely to persist into the future. Although the influence of these Indo-Pacific climate modes on basin precipitation has been demonstrated (Ashok et al., 2004, 2001; Ashok and Saji, 2007; Saji et al., 1999; Kumar et al., 1999; Wu and Wang, 2002), there is considerable uncertainty regarding the spatial distribution and timing of precipitation extremes (Toreti et al., 2013). However, clear understanding of the spatial and seasonal dynamics of basin precipitation is vital because climate modes affect water resources

NHESSD
2, 1671–1692, 2014

CC BY

and the Indian monsoon is expected, under warmer climates, to exhibit weaker circulation, which will lead to more extreme precipitation (Stocker et al., 2013).

Our objective is twofold. First, we analyze where in each basin and at what time of the year precipitation is affected by one or both of the climate modes. Second, we assess how the spatio-temporal variations in precipitation link to the flooding and drought occurrences in each basin as a result of climate mode forcings. This information is critical to establish seasonal predictions of flooding and drought both for the near term and for projected climates.

2 Study basins

The vast system of the Ganges (longitude 73° to 88° East and latitude 22° to 32° North) and Brahmaputra (longitude 82° to 98° East, and latitude 23° to 32° North) river basins has a drainage area of 1.65 million km^2, spanning from the floodplains to the mountainous areas of Nepal, Indian, China, Bhutan and Bangladesh. The basins are physiographically diverse and ecologically rich in natural and crop-related biodiversity. Around 55 % of the combined basin area is modified for cropland, of which 22 % is irrigated. While the Ganges basin is more extensively cultivated (71 % cropland, 15 % irrigated), the Brahmaputra basin is more intensively cultivated (29 % cropland, 47 % irrigated) (Revenga et al., 1998). Water is the single most important natural resource of the basins' over half a billion population who rely on precipitation and snowmelt for their livelihoods and ecosystem services. Water availability in the basins is driven by summer and winter monsoons. The average annual precipitation for the Ganges and Brahmaputra is 1550 mm and 2025 mm respectively (Mirza, 2011). As illustrated in Fig. 1, the basins exhibit wide spatial and temporal variations in precipitation as the basins belong to the monsoon region, where 70–80 % of annual precipitation is concentrated in the June to September months of the summer monsoon (Mirza, 2011). Modulated by ENSO and Indian Ocean Dipole, this unequal spatial and temporal distribution of monsoon precipitation creates recurrent natural hazards of flooding and drought in parts

NHESSD
2, 1671–1692, 2014

of the basins causing damage to life, property, and infrastructure. Documenting where and when precipitation in the basins is modulated by the interactive influence of these climate modes is an important step toward minimizing natural hazard risks and climate impacts under changing climate.

3 Methods and data used

We extracted daily precipitation data at 43 stations (Fig. 1) from the Global Surface Summary of Day (GSOD) dataset (NOAA, 2001) for the period 1982 to 2010, excluding 2002 due to missing records. The daily precipitation values were spatially interpolated employing the inverse distance weighting (IDW) method at 10 km × 10 km resolution to create a continuous field of daily basin wide precipitation. The IDW method is preferred over more spatially informed methods like kriging or co-kriging because our initial tests yielded no significant improvements from geo-interpolated results given the sparsely distributed precipitation locations over the large basin area. The daily precipitation surface grids were summarized to monthly values. Using 28 yr of monthly grids, climatology and annual anomalies were produced. Simultaneously, daily time series for stations in each basin were averaged to create two daily precipitation time series: one for the Ganges basin and another for the Brahmaputra. The daily values were summarized to monthly values, and the climatology and monthly anomalies were computed.

To analyze how precipitation anomalies were modulated by positive and negative IO DMIs, El Niño, or La Niña, we averaged the spatial and monthly anomalies for the years classified in Table 1 and Table 2. These tables are adapted from (Pervez and Henebry, 2013), where details on the classification method are described.

NHESSD
2, 1671–1692, 2014

cc BY

4 Results and discussion

4.1 Spatial variation

Anomalously dry conditions dominated most parts of both basins during El Niño and during the co-occurrence of El Niño and the positive phase of $DMI_{west–east}$ or El Niño and the positive phase of $DMI_{north–south}$(Fig. 2a and b). During El Niño, northwestern India – Uttarakhand, Haryana, and western Uttar Pradesh – in the Ganges basin experienced reductions in precipitation in excess of 81 mm month^{-1} (73 % of the mean), and Arunachal Pradesh and central and western Assam in the Brahmaputra basin experienced reductions in precipitation in excess of 77 mm month^{-1} (47 % of the mean). These areas are the wettest in these basins, and the climatological expectation for precipitation exceeds 110 mm month^{-1} in the Ganges and 162 mm month^{-1} in the Brahmaputra basin. Although Rajasthan, central and eastern Uttar Pradesh, eastern Bihar, and western West Bengal experienced a lesser reduction in precipitation (45 mm month^{-1}, 46 % of the mean) during El Niño, the impacts of El Niño were stronger since these areas are drier and receive less precipitation (97 mm month^{-1}) than northwest India. These areas are also the most agriculturally extensive in the Ganges basin and rely on precipitation for successful agricultural production (Thenkabail et al., 2009). However, precipitation remained close to the average in Jharkhand and western Bihar in the Ganges basin and in northwestern Bangladesh and eastern West Bengal in the Brahmaputra basin during the El Niño years and in the western West Bengal region of the Ganges basin during the co-occurrence of El Niño and a positive $DMI_{west–east}$ mode. During El Niño, surface winds weakened and outgoing longwave radiation (OLR) increased over the Arabian Sea and Indian sub-continent, Bay of Bengal, and the eastern equatorial IO (Pervez and Henebry, 2013). Below average surface winds and suppressed convection contributed to weaken the Walker and Hadley circulations, causing below average precipitation in the basins.

In contrast, consistently wet conditions occurred in both basins during the co-occurrence of La Niña and positive phases of $DMI_{west–east}$ and $DMI_{north–south}$, leading to

NHESSD
2, 1671–1692, 2014

CC BY

substantially above average precipitation across the basins (Fig. 2h). During wet conditions, Uttarakhand, Haryana, eastern Bihar, western West Bengal, and far Western, Central, and Eastern regions of Nepal experienced an increase of over 78 mm month^{-1} (80 % of the mean) in precipitation, but increased precipitation was relatively less in Uttar Pradesh and western Bihar in the Ganges basin. In the Brahmaputra, the largest increase in precipitation (68 mm month^{-1}, 57 % of the mean) appeared over central Assam, eastern West Bengal, and northwestern Bangladesh. During the co-occurrence of La Niña and positive phases of DMI$_{\text{west–east}}$ and DMI$_{\text{north–south}}$, the Walker and Hadley circulations were well developed because of anomalously high wind accompanied by enhanced convection activities and cloud coverage due to anomalously negative OLR over the Arabian Sea, western IO, eastern IO, and the Bay of Bengal (Pervez and Henebry, 2013). As a result, precipitation increased in both basins.

During a neutral influence of El Niño and La Niña accompanied by neutral IO DMI phases, when precipitation was observed to be marginal in most parts of the basins owing to a moderately developed Walker circulation, deficit precipitation may still prevail in the intensive agricultural regions of Jharkhand, Bihar, and Eastern regions of Nepal in the Ganges basin, and in northern Bangladesh, eastern West Bengal, and Assam in the Brahmaputra basin (Fig. 2d). During the study period, neutral years for the ENSO and IO DMI phases prevailed a majority of the time combined for both basins (46 % of the time – five common years, and eight separate years). In the Ganges basin, out of eight neutral years, precipitation was below average in four years (50 % of the time), while in the Brahmaputra basin, out of ten neutral years, precipitation was below average in three years (30 % of the time). This situation is important from an agricultural perspective, implying that a water deficit can likely occur regularly with potentially damaging consequences to the agricultural sector.

During positive DMI$_{\text{west–east}}$, precipitation increased across the Ganges basin, except in eastern Bihar, western West Bengal, and the Eastern region of Nepal by 17 mm month^{-1} (17 % of the mean) (Fig. 2e). During a positive DMI$_{\text{north–south}}$ mode, while precipitation increased slightly (4 mm month^{-1}, 3 % of the mean) in northern

NHESSD
2, 1671–1692, 2014

Bangladesh and Arunachal Pradesh, it remained close to average in Assam and below average in the Tibetan Plateau and Bhutan. The influences of La Niña result in two different scenarios for Ganges and Brahmaputra basin precipitation. While precipitation remained average in the Ganges, except for Uttarakhand, central Uttar Pradesh, and Madhya Pradesh, substantial reductions (23 mm month^{-1}, 20 % of the mean) in precipitation were observed in the Brahmaputra basin, especially in the west (Fig. 2g). Substantial reductions in precipitation during a negative $\mathrm{DMI}_{\text{west–east}}$ mode (32 mm month^{-1}, 32 % of the mean) and co-occurrence of the same with La Niña (19 mm month^{-1}, 19 % of the mean) were also seen across the Ganges basin (Fig. 2c and f).

4.2 Seasonal variation

Typically, the IO dipole starts to develop in May–June and peaks in October, followed by a rapid demise (Saji et al., 1999). Therefore, the influence of both ENSO and IO dipole modes was most prominent during the monsoon months (June through September). The high precipitation during the monsoon months in both basins was apparent, as shown in Figs. 3 and 4. For dry conditions, during El Niño and the co-occurrence of El Niño and a positive IO $\mathrm{DMI}_{\text{west–east}}$ mode, peak monsoon precipitation reduced to around 221 mm month^{-1} for July and August in the Ganges basin. The basin precipitation reduced to 60 % of the baseline (baseline is defined as all neutral years' monsoon precipitation, Table 1) during El Niño, and 77 % of the baseline during the co-occurrence of El Niño and a positive $\mathrm{DMI}_{\text{west–east}}$ mode. Although the seasonal cycle of precipitation under El Niño events was not statistically significantly different from the cycle of dry conditions, it was below the expected mean of the dry conditions during El Niño (Fig. 3a), and slightly above the expected mean of the dry conditions during the co-occurrence of El Niño and a positive $\mathrm{DMI}_{\text{west–east}}$ mode (Fig. 3b). In the Brahmaputra basin, peak monsoon precipitation reduced to 170 mm month^{-1} for July and August under dry conditions. El Niño events significantly decreased August precip-

NHESSD
2, 1671–1692, 2014

CC BY

itation, while co-occurrence of El Niño and a positive IO $DMI_{north–south}$ mode enhanced August precipitation, but not statistically significant (Fig. 4a and b). Around 88 % and 100 % of baseline precipitation (Table 2) was observed during sole El Niños and during co-occurrences of El Niño and a positive $DMI_{north–south}$ mode in the Brahmaputra basin.

For neutral conditions, occurrence of a negative $DMI_{west–east}$ mode reduced the monsoon precipitation statistically significantly (Fig. 3c), whereas a positive $DMI_{west–east}$ mode enhanced monsoon precipitation, especially during the peak months of July and August in the Ganges basin (Fig. 3e). The peak monsoon precipitation rose to 270 mm month^{-1} during all neutral conditions in the Ganges basin. In the Brahmaputra basin, around 185 mm month^{-1} of precipitation was observed during the peak monsoon month under all neutral conditions with little difference in the seasonal cycle during a positive $DMI_{north–south}$ mode (Fig. 4c and d).

For wet conditions, co-occurrence of La Niña and a positive $DMI_{west–east}$ produced a statistically significantly enhanced seasonal cycle – both in terms of duration and magnitude – with consistently high precipitation throughout the year, peaking in July at ~ 400 mm month^{-1} in the Ganges basin (Fig. 3h). In the Brahmaputra basin, the co-occurrence of La Niña and a positive $DMI_{north–south}$ statistically significantly enhanced June and July precipitation (averaging 285 mm month^{-1}) (Fig. 4f). Ganges precipitation increased to 135 % of the baseline, and Brahmaputra precipitation increased to 160 % of the baseline during the co-occurrence of La Niña and positive IO dipole modes. The sole occurrence of La Niña or the combination of La Niña with negative IO dipole modes reduced precipitation statistically significantly, especially during the pre-monsoon months in both basins (Figs. 3f, g, and 4e).

4.3 Implications for flooding and drought

Monsoon precipitation is the primary cause for flooding in these basins, especially downstream across Bangladesh (Webster et al., 2010). In 1987, 1988, and 1998, extensive flooding occurred downstream when both rivers crested simultaneously (Webster et al., 2010). In 1987, despite prevailing dry conditions due to the co-occurrence

CC BY

of El Niño and positive DMIs, severe flooding was observed both in the Ganges and Brahmaputra basins (Table 3). The year 1988, when La Niña prevailed, was characterized as a wet year for both basins. While 1998 was a wet year for the Ganges basin influenced by the co-occurrence of La Niña and negative $\mathrm{DMI}_{\text{west–east}}$, it was a neutral year for the Brahmaputra basin influenced by a developing La Niña and positive $\mathrm{DMI}_{\text{north–south}}$. In 2004, 2007, and 2008, flooding (Table 3) occurred in the Brahmaputra basin only (Webster et al., 2010). The years 2004 and 2008 were neutral for the Brahmaputra basin. Precipitation was influenced by positive $\mathrm{DMI}_{\text{north–south}}$ in 2004 with expected above average precipitation in northern Bangladesh, Assam, and Arunachal Pradesh with possibilities of flooding downstream. While no climate mode influence was active in 2008, below average precipitation was expected along the downstream parts of the basin; however, above average precipitation was possible over Assam and Arunachal Pradesh (Fig. 2d) with possibilities of flooding downstream. The year 2007 was a wet year when precipitation was influenced by the co-occurrence of La Niña and positive $\mathrm{DMI}_{\text{north–south}}$, leading to above average precipitation (Table 2, Fig. 2h). There was major flooding in the far upstream parts of the Ganges basin and in the Indus basin in Pakistan in 2010 (Mujumdar et al., 2012). The year 2010 was a wet year in the Ganges influenced by La Niña alone. However, the flooding in the upper reaches of the Ganges in 2010 was not experienced downstream (IFRC, 2010).

Drought is another natural hazard common to parts of both basins. In 1989 and 1992 (Table 3), drought conditions prevailed in the lower reaches of the Ganges basin, and in 1982, 1986, and 1994 (Table 3), drought prevailed in the Brahmaputra basin (Chowdhury and Ward, 2007). Below average precipitation dominated much of the Ganges basin in 1989 and 1992 under the strong influence of a negative $\mathrm{DMI}_{\text{west–east}}$ mode alone. For Brahmaputra, 1982 was an El Niño year when below average precipitation was expected. In contrast, 1986 and 1994 were neutral years when below average precipitation prevailed in the eastern part of the Ganges basin and across the Brahmaputra basin without any apparent influence from climate modes (Fig. 2d).

NHESSD
2, 1671–1692, 2014

cc BY

In general, major flooding and drought occurred in the basins in accordance with the expected above or below average precipitation due to the prevailing influence of ENSO and the IO dipoles. However, major flooding was observed during El Niño years when below average precipitation was expected. During the past few decades, increasing trends of extreme heavy precipitation events have been observed (Rajeevan et al., 2008; Stocker et al., 2013). Monsoon precipitation has been increasing especially in the Ganges basin (Moors et al., 2011), but precipitation amounts before and after the monsoon have been declining (Ramesh and Goswami, 2007), and the number of rainy days has been declining (Das et al., 2013). As suggested by these studies, when precipitation increases over a shorter period of time with a reduced number of rain days, flash flooding is expected regardless of the influence by the climate modes.

5 Conclusion

We have documented where and when precipitation in the Ganges and Brahmaputra basins have been modulated by the influence of ENSO and the dipole modes in the Indian Ocean singly and in tandem. Importantly, deficit precipitation prevails across the basins during El Niño, especially in Uttarakhand, Haryana, and western Uttar Pradesh in the Ganges basin, and in Arunachal Pradesh, and central and western Assam in the Brahmaputra basin. The combined influence of La Niña and positive IO $DMI_{west–east}$ and $DMI_{north–south}$ produces the most precipitation over both basins. The occurrence of El Niño alone and co-occurrence of La Niña and positive IO DMI phases produce extreme dry and wet precipitation regimes, respectively. However, their frequency is limited.

Perhaps the most compelling observation is that during neutral years, which occurred most frequently (46 % of the time during the study period), below average precipitation may prevail in Jharkhand, Bihar, and eastern regions of Nepal in the Ganges, and in northern Bangladesh, eastern West Bengal, and Assam in the Brahmaputra basin, while below average to average precipitation may prevail in the agriculturally exten-

CC BY

sive areas of Haryana and Uttar Pradesh. The occurrence of more frequent neutral years shapes the requirements for successful agricultural production by supplemental irrigation from declining groundwater sources (61 % of irrigation water comes from groundwater) (UNEP, 2009; Rodell et al., 2009). This pattern implies that agricultural production is challenging, even in the neutral years or years with the influence of positive IO DMI phases when average precipitation is expected, because of evident scarcity of water resources.

At the seasonal scale, in wet years during the co-occurrence of La Niña and positive IO DMI phases, precipitation increased statistically significantly in almost every month of the year in the Ganges basin, but in the Brahmaputra basin the increased precipitation was noticeable from May through August. In dry years, El Niño tends to reduce precipitation in peak monsoon months – July and August – while a positive $\mathrm{DMI}_{\text{west–east}}$ mode minimized the effects of El Niño when they co-occurred in the Ganges basin. In the Brahmaputra basin, the precipitation in the pre-monsoon months of April and May and peak monsoon month of August was statistically significantly reduced by El Niño, and these impacts were also minimized during the co-occurrence of El Niño and a positive $\mathrm{DMI}_{\text{north–south}}$ mode. When La Niña co-occurred with positive IO DMI phases, it increased the precipitation in both basins. Although confidence intervals are helpful in identifying the nature of seasonal modulation in the precipitation regime, they may underestimate precipitation variability, since the number of years observed was low for some climate mode combinations.

We have noted occurrences of major flooding and drought as consequences of the interactive effects of ENSO and IO dipoles. However, there are other years with similar influences by the ENSO and/or IO DMI phases that did not produce flooding or drought. This finding implies that other factors, in addition to the climate mode influences, affect the timing and location of precipitation to produce flooding or drought in the basins. Although the length of the observational record for interactive effects of ENSO and IO DMI phases on basin precipitation was relatively brief, the spatial and temporal precipitation response identified where and when the climate modes modulate precipitation

NHESSD
2, 1671–1692, 2014

cc BY

in the basins. This information is critical for the development of early warning of natural hazard risks and may provide information to support the development of local strategies to minimize climate mode impacts on agricultural production and rural livelihoods.

Acknowledgements. This research was supported in part by the US Agency for International Development Famine Early Warning Systems Network agreement with the US Geological Survey, and in part by the Geospatial Sciences Center of Excellence at South Dakota State University. We thank these agencies for their support. We sincerely thank Gabriel Senay, James P. Verdin, James Rowland and Michael Budde at USGS EROS for suggestions made throughout the research. We greatly appreciate the astute comments made by the anonymous reviewers, and by USGS reviewers which helped us improve the manuscript considerably.

References

Ashok, K. and Saji, N. H.: On the impacts of ENSO and Indian Ocean dipole events on sub-regional Indian summer monsoon rainfall, Nat. Hazards, 42, 273–285, 2007.

Ashok, K., Guan, Z., and Yamagata, T.: Impact of the Indian Ocean dipole on the relationship between the Indian monsoon rainfall and ENSO, Geophys. Res. Lett., 28, 4499–4502, 2001.

Ashok, K., Guan, Z., Saji, N. H., and Yamagata, T.: Individual and combined influences of ENSO and the Indian Ocean Dipole on the Indian summer monsoon, J. Climate, 17, 3141–3155, 2004.

Chowdhury, M. R. and Ward, M. N.: Hydro-meteorological variability in the greater Ganges-Brahmaputra-Meghna basins, Int. J. Climatol., 24, 1495–1508, 2004.

Chowdhury, M. R. and Ward, M. N.: Seasonal flooding in Bangladesh – variability and predictability, Hydrol. Process., 21, 335–347, 2007.

Das, P. K., Chakraborty, A., and Seshasai, M. V. R.: Spatial analysis of temporal trend of rainfall and rainy days during the Indian Summer Monsoon season using daily gridded ($0.5^{\circ} \times 0.5^{\circ}$) rainfall data for the period of 1971–2005, Meteorol. Appl., 1361, doi:10.1002/met.1361, 2013.

IFRC: Bangladesh: Flash Flood International Federation of Red Cross and Red Crescent Societies, Inf. Bull. No. 1, Geneva, Switzerland, 2010.

Kumar, K. K., Rajagopalan, B., and Cane, M. A.: On the weakening relationship between the Indian monsoon and ENSO, Science, 284, 2156–2159, 1999.

Mirza, M. Q.: Climate Change, flooding in South Asia and implications, Environ. Change, 11, 95–107, 2011.
Moors, E. J., Groot, A., Biemans, H., Van Scheltinga, C. T., Siderius, C., Stoffel, M., Huggel, C., Wiltshire, A., Mathison, C., Ridley, J., Jacob, D., Kumar, P., Bhadwal, S., Gosain, A., and Collins, D. N.: Adaptation to changing water resources in the Ganges Basin, northern India, Environ. Sci. Policy, 14, 758–769, 2011.
Mujumdar, M., Preethi, B., Sabin, T. P., Ashok, K., Saeed, S., Pai, D. S., and Krishnan, R.: The Asian summer monsoon response to the La Niña event of 2010, Meteorol. Appl., 19, 216–225, 2012.
Pervez, M. S. and Henebry, G. M.: Dipole modes in the Indian Ocean linked to the Ganges and Brahmaputra precipitation anomalies., Environ. Res. Lett., in review, 2013.
Rajeevan, M., Bhate, J., and Jaswal, A. K.: Analysis of variability and trends of extreme rainfall events over India using 104 years of gridded daily rainfall data, Geophys. Res. Lett., 35, L18707, doi:10.1029/2008GL035143, 2008.
Ramesh, K. V. and Goswami, P.: Reduction in temporal and spatial extent of the Indian summer monsoon, Geophys. Res. Lett., 34, L23704, 2007.
Revenga, C., Murray, S., Abramovitz, J., and Hammond, A.: Watersheds of the World: Ecological Value and Vulnerability, World Resources Institute and Worldwatch Institute, Washington DC, 1998.
Rodell, M., Velicogna, I., and Famiglietti, J. S.: Satellite-based estimates of groundwater depletion in India, Nature, 460, 999–1002, 2009.
Ropelewski, C. F. and Halpert, M. S.: Quantifying southern oscillation-precipitation relationships, J. Climate, 9, 1043–1059, 1996.
Saji, N. H., Goswami, B. N., Vinayachandran, P. N., and Yamagata, T.: A dipole mode in the tropical Indian Ocean, Nature, 401, 360–363, 1999.
Stocker, T., Dahe, Q., Plattner, G., Alexander, L., Allen, S., Bindoff, N., Breon, F., Church, J., Cubasch, U., Emori, S., Forster, P., Friedlingsteri, P., Gillett , N., Gregory, J., Hartmann, D., Jansen, E., Kirtman, B., Knutti, R., Kanikicharla, K. K., Lemke, P., Marotzke, J., Delmotte, V. M., Meehl, G., Mokhov, I., Piao, S., Ramaswamy, V., Randall, D., Rhein, M., Rojas, M., Sabine, C., Shindell, D., Talley, L., Vaughan, D., and Xia, P.: Working Group I Contribution to the IPCC Fifth Assessment Report, Climate change 2013: the physical science basis, Intergovernmental Panel on Climate Change, released 26 September, Stockholm, Sweden, 2013.

NHESSD
2, 1671–1692, 2014

Spatial and seasonal responses of precipitation

M. S. Pervez and G. M. Henebry

Title Page
Abstract | Introduction
Conclusions | References
Tables | Figures
◀◀ | ▶▶
◀ | ▶
Back | Close
Full Screen / Esc
Printer-friendly Version
Interactive Discussion

CC BY

Thenkabail, P. S., Biradar, C. M., Noojipady, P., Dheeravath, V., Li, Y., Velpuri, M., Gumma, M., Gangalakunta, O. R. P., Turral, H., Cai, X., Vithanage, J., Schull, M. A., and Dutta, R.: Global Irrigated Area Map (GIAM), derived from remote sensing, for the end of the last millennium, Int. J. Remote Sens., 30, 3679–3733, 2009.

Toreti, A., Naveau, P., Zampieri, M., Schindler, A., Scoccimarro, E., Xoplaki, E., Dijkstra, H. A., Gualdi, S., and Luterbacher, J.: Projections of global changes in precipitation extremes from Coupled Model Intercomparison Project Phase 5 models, Geophys. Res. Lett., 40, 4887–4892, 2013.

UNEP: Chief Liquidity Series, Water-related materiality briefings for financial institutions, United Nations Environment Programme, Switzerland, 2009.

Webster, P. J., Moore, A. M., Loschnigg, J. P., and Leben, R. R.: Coupled ocean-atmosphere dynamics in the Indian Ocean during 1997–98, Nature, 401, 356–360, 1999.

Webster, P. J., Jian, J., Hopson, T. M., Hoyos, C. D., Agudelo, P. A., Chang, H. R., Curry, J. A., Grossman, R. L., Palmer, T. N., and Subbiah, A. R.: Extended-range probabilistic forecasts of Ganges and Brahmaputra floods in Bangladesh, B. Am. Meteorol. Soc., 91, 1493–1514, 2010.

Wu, R. and Wang, B.: A contrast of the East Asian summer monsoon-ENSO relationship between 1962–77 and 1978–93, J. Climate, 15, 3266–3279, 2002.

NHESSD

2, 1671–1692, 2014

Spatial and seasonal responses of precipitation

M. S. Pervez and G. M. Henebry

CC BY

Table 1. Classification of years based on occurrence, co-occurrence, or absence of climate mode ($DMI_{west–east}$, ENSO) extremes. Precipitation values are averaged over the July through November period, with the baseline being the observed precipitation during the absence of climate mode extremes (neutral years). In no year was the co-occurrence of El Niño and negative $DMI_{west–east}$ observed for the Ganges basin.

[El Niño and negative $DMI_{west–east}$] No years observed	[El Niño] 1987 avg: 568 mm 60 % of baseline	[El Niño and positive $DMI_{west–east}$] 1982, 1997 avg: 731 mm 77 % of baseline
[negative $DMI_{west–east}$] 1989, 1992, 1996 avg: 650 mm 68 % of baseline	[Neutral] 1983, 1986, 1990, 1993, 1995, 2000, 2001, 2004, 2005, 2009 baseline: 946 mm	[Positive $DMI_{west–east}$] 1991, 1994, 2003, 2006, 2008 avg: 1056 mm 112 % of baseline
[La Niña and negative $DMI_{west–east}$] 1984, 1985, 1998 avg: 775 mm 82 % of baseline	[La Niña] 1988, 2010 avg: 1035 mm 109 % of baseline	[La Niña and positive $DMI_{west–east}$] 1999, 2007 avg: 1277 mm 135 % of baseline

NHESSD
2, 1671–1692, 2014

Table 2. Classification of years based on occurrence, co-occurrence, or absence of climate mode ($DMI_{north–south}$, ENSO) extremes. Brahmaputra precipitation values are averaged over the July through November period, with the baseline being the observed precipitation during the absence of climate mode extremes (neutral years). In no year was the co-occurrence of El Niño/La Niña and negative $DMI_{north–south}$ observed for the Brahmaputra basin.

[El Niño and negative $DMI_{north–south}$] No years observed	[El Niño] 1982, 1997 avg: 609 mm 88 % of baseline	[El Niño and positive $DMI_{north–south}$] 1983, 1987, 2006, 2009 avg: 690 mm 100 % of baseline
[Negative $DMI_{north–south}$] No years observed	[Neutral] 1984, 1985, 1986,1990, 1991, 1993,1994, 1996, 2001, 2008 baseline: 688 mm	[Positive $DMI_{north–south}$] 1989, 1992, 1995, 1998 2003, 2004, 2005 avg: 796 mm 115 % of baseline
[La Niña and negative $DMI_{north–south}$] No years observed	[La Niña] 1988 avg: 620 mm 90 % of baseline	[La Niña and positive $DMI_{north–south}$] 1999, 2000, 2007, 2010 avg: 1101 mm 160 % of baseline

NHESSD
2, 1671–1692, 2014

CC BY

Table 3. List of major droughts and floods in the Ganges and Brahmaputra basins under interactive influence of ENSO and IO dipole modes during 1982–2010. The unlisted years were neutral, with no major droughts and floods in either basin.

Ganges	Year	El Niño	La Niña	Pos. DMI_{we}	Neg. DMI_{we}	Major Drought	Major Flood
Dry	1982	•		•			
	1987	•					×
	1997	•		•			
Neutral	1989				•	×	
	1991			•			
	1992				•	×	
	1994			•			
	1996				•		
	2003			•			
	2006			•			
	2008			•			
Wet	1984		•		•		
	1985		•		•		
	1988		•				×
	1998		•		•		×
	1999		•	•			
	2007		•	•			
	2010		•				×

Brahmaputra	year	El Niño	La Niña	Pos. DMI_{ns}	Neg. DMI_{ns}	Major Drought	Major Flood
Dry	1982	•				×	
	1983	•		•			
	1987	•		•			×
	1997	•					
	2006	•		•			
	2009	•		•			
Neutral	1986					×	
	1989			•			
	1992			•			
	1994					×	
	1995			•			
	1998			•			×
	2003			•			
	2004			•			×
	2005			•			
	2008						×
Wet	1988		•				×
	1999		•	•			
	2000		•	•			
	2007		•	•			×
	2010		•	•			

NHESSD
2, 1671–1692, 2014

Spatial and seasonal responses of precipitation

M. S. Pervez and G. M. Henebry

CC BY

NHESSD
2, 1671–1692, 2014

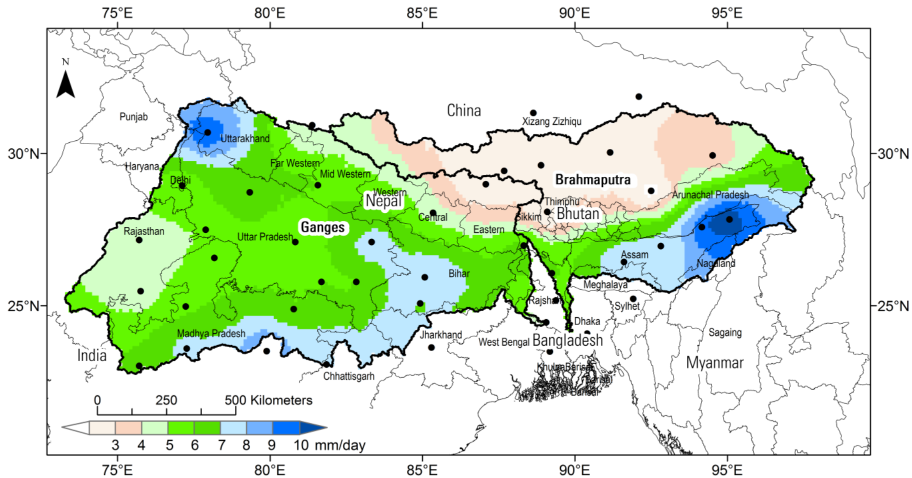

Fig. 1. The Ganges and the Brahmaputra river basins overlaid by the administrative boundaries and observed precipitation station locations. The precipitation climatology (1982–2010) is shown in the background colors.

CC BY

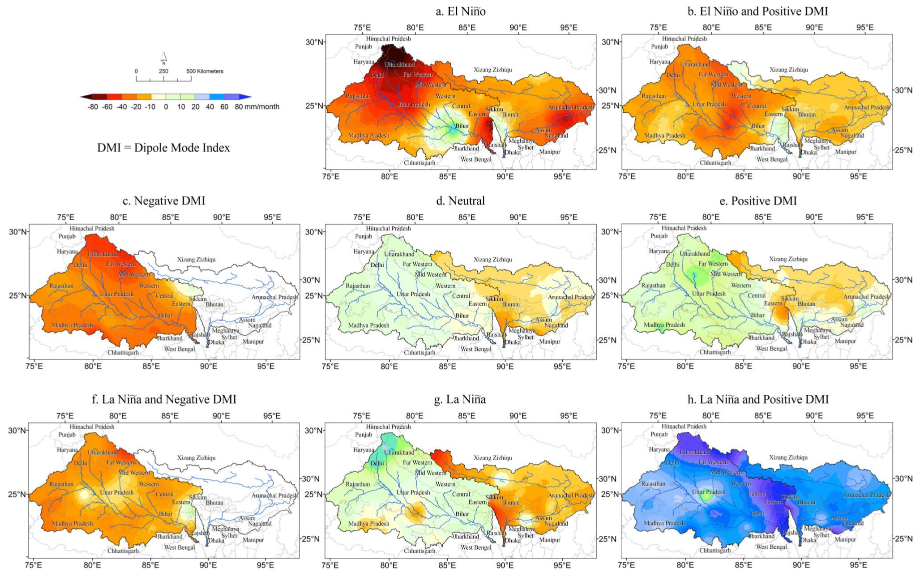

Fig. 2. Precipitation anomalies (mm month^{-1}) based on occurrence, co-occurrence, or absence of climate mode (dipole modes, ENSO) extremes. $DMI_{west–east}$ was used for the Ganges basin while $DMI_{north–south}$ was used for the Brahmaputra basin in classifying the years. No years with the co-occurrence of El Niño and negative $DMI_{west–east}$ were observed for the Ganges basin, and no years with the co-occurrence of El Niño/La Niña and negative $DMI_{north–south}$ were observed for the Brahmaputra basin during the study period (1982–2010).

NHESSD
2, 1671–1692, 2014

CC BY

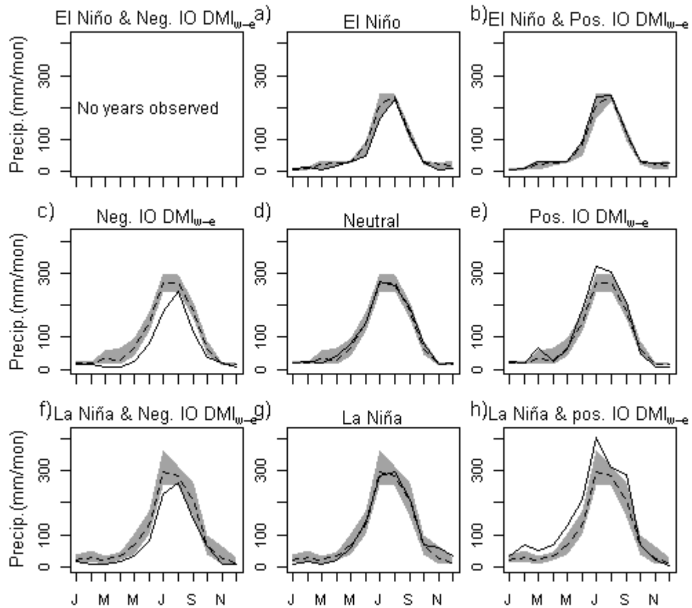

Fig. 3. Temporal variation in the Ganges basin monthly precipitation ($mm\,month^{-1}$) under the influence of different climate modes. The seasonal cycle is shown for the period 1982–2010. The dashed black line reproduces expected mean during dry conditions in **(a, b)**, neutral conditions in **(c, d, e)**, and wet conditions in **(f, g, h)**. The solid black line is the mean for the respective climate modes marked in each plot, and the grey shading is the 90 % confidence levels determined through 1000 samples in bootstrapping technique using percentile and bias corrected and accelerated (BCa) method. Solid black line outside the grey-shaded area indicates that the values are significantly different from expected values under dry, neutral, or wet conditions. Dry condition is defined by El Niño (co-)occurrence with positive IO dipole modes, neutral condition is defined by moderate to no influence of ENSO and IO dipole modes, and wet condition is defined by La Niña (co-)occurrence with positive or negative IO dipole modes. The combined influence of El Niño and negative $DMI_{west-east}$ was not observed on the Ganges precipitation during the study period. DMI: Dipole Mode Index.

NHESSD
2, 1671–1692, 2014

Spatial and seasonal responses of precipitation

M. S. Pervez and G. M. Henebry

Title Page
Abstract
Introduction
Conclusions
References
Tables
Figures
◂
▸
Back
Close
Full Screen / Esc
Printer-friendly Version
Interactive Discussion

CC BY

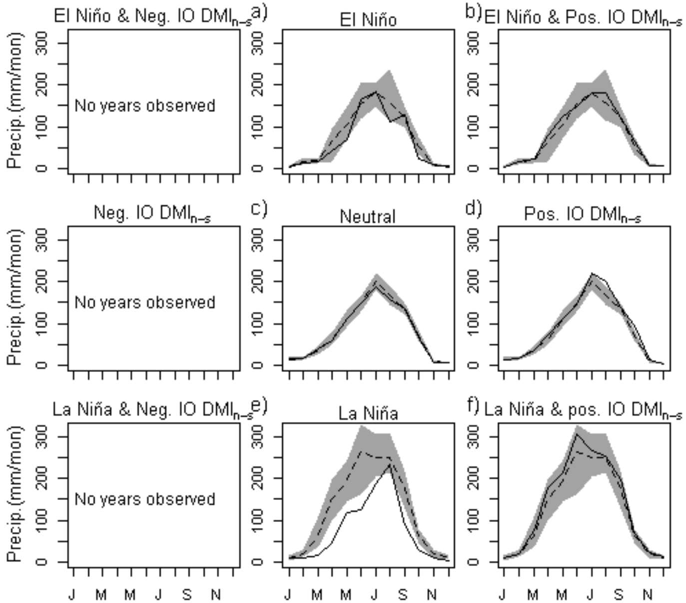

Fig. 4. Temporal variation in the Brahmaputra basin monthly precipitation (mm month^{-1}) under the influence of different climate modes. The seasonal cycle is shown for the period 1982–2010. The dashed black line reproduces expected mean during dry conditions in **(a, b)**, neutral conditions in **(c, d)**, and wet conditions in **(e, f)**. The solid black line is the mean for the respective climate modes marked in each plot, and the grey shading is the 90 % confidence levels determined through 1000 samples in bootstrapping technique using percentile and bias corrected and accelerated (BCa) method. Solid black line outside the grey-shaded area indicates that the values are significantly different from expected values under dry, neutral, or wet conditions. Dry condition is defined by El Niño (co-)occurrence with positive IO dipole modes, neutral condition is defined by moderate to no influence of ENSO and IO dipole modes, and wet condition is defined by La Niña (co-)occurrence with positive or negative IO dipole modes. The combined influence of negative $DMI_{north–south}$ with El Niño or La Niña was not observed on the Brahmaputra precipitation during the study period. DMI: Dipole Mode Index.

NHESSD

2, 1671–1692, 2014

CC BY